Chemical Papers (2024) 78:3507–3514
https://doi.org/10.1007/s11696-024-03324-6

ORIGINAL PAPER

Toxicity of energetic nanomaterials assessed on L929 fibroblasts

Sijia Liu[1,2] · Can Tang[1,2] · Kai Jiang[1] · Liyuan Zhang[1] · Nan Ma[2] · Yang Li[2] · Meikun Fan[2] · Bing Huang[1]

Received: 12 December 2023 / Accepted: 12 January 2024 / Published online: 15 February 2024

Abstract

The widespread use of energetic materials (EMs) has increased human exposure to these substances, and the potential toxicity of nano-sized EMs remains a largely unexplored area of research. This study investigates the cytotoxicity of three nano-sized energetic nanomaterials, namely nano-sized triaminotrinitrobenzene (nano-TATB), hexanitrostilbene (HNS-IV), and 2,6-diamino-3,5-dinitropyrazine-1-oxide (nano-LLM-105), using L929 fibroblasts for in vitro testing. The findings demonstrate a significant dose-dependent toxic effect on L929 cells. As the dose increases, cell density decreases, cell morphology becomes rounder, and cell gaps widen. The results of cell activity assays, lactate dehydrogenase (LDH) and superoxide dismutase (SOD) activity measurements, and apoptosis detection suggest that the cytotoxicity is caused by cell membrane fragmentation and the excessive production of reactive oxygen species (ROS), leading to oxidative stress. Given the potential for EMs to cause toxic effects in various tissues and organs, including the liver and kidneys, and even teratogenic and mutagenic effects, this work provides valuable insights into the toxicological evaluation of energetic nanomaterials.

Keywords L929 fibroblast · Cytotoxicity · Energetic materials · Nanomaterial · Toxicological study

Abbreviations

EMs	Energetic materials
nano-TATB	Nano-sized triaminotrinitrobenzene
HNS-IV	Hexanitrostilbene
nano-LLM-105	2,6-Diamino-3,5-dinitropyrazine-1-oxide
LDH	Lactate dehydrogenase
SOD	Superoxide dismutase
ROS	Reactive oxygen species
RGO	Reduced graphene oxide
GO	Graphene oxide

Introduction

Energetic materials (EMs) are a class of materials in which a large amount of chemical energy is stored and can be released. It occupies an important position in military explosives, fuels, and rocket propellants (Badgujar et al. 2008; Du et al. 2021; Gao et al. 2020). For example, trinitrotoluene (TNT), nitroglycerine (NG), hexogen (RDX), and octogen (HMX) are probably the most well-known ones. In fact, nano-sized triaminotrinitrobenzene (nano-TATB), hexanitrostilbene (HNS-IV), and 2,6-diamino-3,5-dinitropyrazine-1-oxide (nano-LLM-105) are the most promising explosives for industrial applications in the field of energetic materials, among which ultrafine HNS-IV has been used in conventional weapons. It has been shown that typical explosives, such as TNT, are toxic to cells (Banerjee et al. 2003), microorganisms (Yang et al. 2021), invertebrates (Berthelot et al. 2008), mammals (Johnson et al. 2017; Skalska and Struzynska 2015), and occupational groups (Wang et al. 2019) to varying degrees (For more specific details refer to Note S1 of the Supplementary Material). In addition, many research studies have shown that nanomaterials (NMs) also exhibit toxicity, accumulate in soil (Wang et al. 2023), and are a threat to the environment (De Matteis et al. 2022; Hartwig and van Thriel 2023; Kim et al. 2012; Qu et al. 2019; Vimbela et al. 2017; Winkless 2023).

The cytotoxicity of nanomaterials may vary depending on the type of cell being exposed (Prasad 2019a, b). For example, TNT has the highest toxicity to Chinese hamster ovary-K1 (CHO) cells., i.e., LC_{50} of 24 μmol L^{-1} (Honeycutt et al. 1996). In contrast, it was the least toxic to hamster

✉ Meikun Fan
meikunfan@gmail.com

✉ Bing Huang
huangtingjun-111@163.com

[1] China Academy of Engineering Physics Institute of Chemical Materials, Mianyang, Sichuan, China

[2] Faculty of Geosciences and Environmental Engineering, Southwest Jiaotong University, Chengdu, Sichuan, China

lung cells V79, i.e., LC_{50} of about 197 μmol L^{-1} (Lachance et al. 1999). Two types of cell lines are usually considered to evaluate the toxicity of certain material in vitro, namely the macrophages and the fibroblasts. The former is the sentinel, which has diverse functions in immunity and repair, while the latter is responsible for tissue structure and integrity (Franklin 2021). Mouse fibroblast L929 cells are the standard cell line for cytotoxicity experiments and are the recommended cell line for YY/T0993-2015 "In Vitro Cytotoxicity Experiment Standard" (He et al. 1999). Currently, there are relatively few studies on the biotoxicity of EMs, with the use of the Vibrio fischeri luminescent bacterial assay to detect different types of EMs such as azidoethanol, 1- and 2-aminotetrazole, etc. (Can et al. 2020; Klapötke et al. 2020).

Various mechanisms for the toxic effects of NMs have been raised. One explanation is that the active surface and small size of the materials allow them to cross cell membranes and interact with different cell structures and biomolecules (Chatterjee et al. 2024; Dev et al. 2017). Specifically, nanoparticles can penetrate biological barriers, accumulate in various organs, and cause toxic effects such as oxidative stress, DNA damage, cell death, and morphological changes (Liu et al. 2018; Mohanty et al. 2022; Wu et al. 2022). Reactive oxygen species (ROS) are formed on nanoparticles or metal ions released from the surface of the particles, interfering with cellular pathways and damaging cellular components and DNA (Atalay et al. 2018). At the same time, the balance between ROS production and antioxidant defense determines the degree of oxidative stress (Finkel & Holbrook 2000). Based on the biotoxicity effects of nanoscale EMs, it is worth further revealing the possible mechanisms.

In this work, we assess the toxicity of three types of energetic nanomaterials on L929 fibroblasts. The nano-sized EMs are nano-TATB, HNS-IV, and nano-LLM-105. By detecting the cell activity after the exposure of nano-sized EMs, we obtain a relationship between the EMs dose and cytotoxicity. Further, we explore the lactate dehydrogenase (LDH) and peroxidase dismutase (SOD) activity, as well as the degree of apoptosis, and propose the possible toxicity mechanism of these nano-sized EMs.

Experimental section

Preparation and purification of nanoscale EMs

Spherical or ellipsoidal nano-TATB quasi-three-dimensional (3D) nano grids, HNS-IV nanoparticles, and nano-sized LLM-105 were synthesized according to the literatures (Wang et al. 2001; Yang et al. 2006; Zhang et al. 2014). See Supporting Information for detailed information on the preparation.

Cell morphological characterization

L929 fibroblasts in the logarithmic growth phase were selected, and the cell density was 1×10^5/mL. 100 μL cellular fluid was then taken in 96-well plates, incubated at 37 °C, and 5% CO_2 at a constant temperature. After cell attachment, three EMs at different concentrations were added to the suspension. Then, the cells were incubated for 24 h, and morphological changes were observed under an inverted microscope.

Detection of cell activity

The cellular activity was usually determined using a chemical reagent method, such as CCK8, which reacts with dehydrogenase in living cells to produce a blue or yellow formazan compound (Mu et al. 2022). Cells in the logarithmic growth phase were selected for a 6×10^4/mL cell density. EMs were added to cells for toxicity reactions. After 24 h of incubation, 200 μL of CCK8 reagent was added to each well. After another 4 h of incubation, the absorbance (A) value at 450 nm was measured by an enzyme marker. The cell activity was calculated as follows.

$$\text{Cell activity} = \frac{A_1 - A_0}{A_2 - A_0} \times 100\%$$

where A_0 is the absorbance of the blank control; A_1 is the absorbance of the experimental group; A_2 is the absorbance of the control group in $L \cdot (g \cdot cm)^{-1}$.

Cell culture supernatant LDH activity assay

We select cells in the logarithmic growth phase and adjust the cell density to 6×10^4/mL. The cultured cells were subjected to toxicity assay and incubated for 24 h according to the above conditions. Then, take the cell supernatant and use the LDH kit to detect LDH viability, and strictly follow the kit instructions.

Detection of cellular oxidative stress

We selected cells in a logarithmic growth phase and adjusted the cell density to 1×10^5/mL. Then, the cell was incubated for 24 h. After removing the supernatant, the cells were collected, and the SOD kit detected their viability.

Detection of apoptosis

L929 cells in the logarithmic growth phase were selected for toxicity assay and cultured for 24 h as described

above, the cells were washed with PBS buffer and then digested with trypsin. Then, the cell liquid was added to a 1.5 mL tube and centrifuged at 1000 rpm for 5 min, and the supernatant was removed. Next, add 500 µL of buffer to resuspend the cells, add five µL of Annexin V-APC/PI to mix well, and then use flow cytometry to detect. The flow cytometer parameters were excitation wavelength Ex = 488 nm, emission wavelength FL1 (Em = 525 ± 20 nm), and FL2 (Em = 585 ± 21 nm). Annexin V-APC green fluorescence was detected through the FITC channel (FL1), and PI red fluorescence was detected through the PI channel (FL2). The percentage of each cell type was counted, and the level of apoptosis was quantitatively analyzed.

Statistical analyses

The data of cell activity and apoptosis levels in this experiment were taken as the mean values of three parallel samples, and the data were expressed in the form of "mean ± standard deviation," and the data were processed by SPSS22.0 software, and the experimental data were counted by one-way ANOVA.

Results and discussion

Cell morphological changes

In Fig. 1, we show the morphological information of L929 cells with an inverted microscope. The morphology of uninfected L929 cells is shown in Fig. 1a, which shows that the cells are in good growth condition and have a long shuttle shape.

It is known that when cells were cultured with the presence of toxic materials, the cell morphology and its proliferation rate could change accordingly. Thus, the changes in cell morphology can be used for preliminary determination of the material's toxicity.

In a relatively low concentration of 5 µg mL^{-1}, the morphology and density of the cells in nano-TATB (Fig. 1b) and HNS-IV (Fig. 1e) stained groups did not change significantly compared with the unstained control group. The results indicate that a low concentration of nano-TATB and HNS-IV did not obviously damage the L929 fibroblasts cell. In contrast, the density of nano-LLM-105 (Fig. 1h) stained cells decreased slightly.

When the concentration was increased to 10 µg mL^{-1}, the cell density of the nano-TATB (Fig. 1c) and HNS-IV (Fig. 1f) contaminated groups also started to decline; the

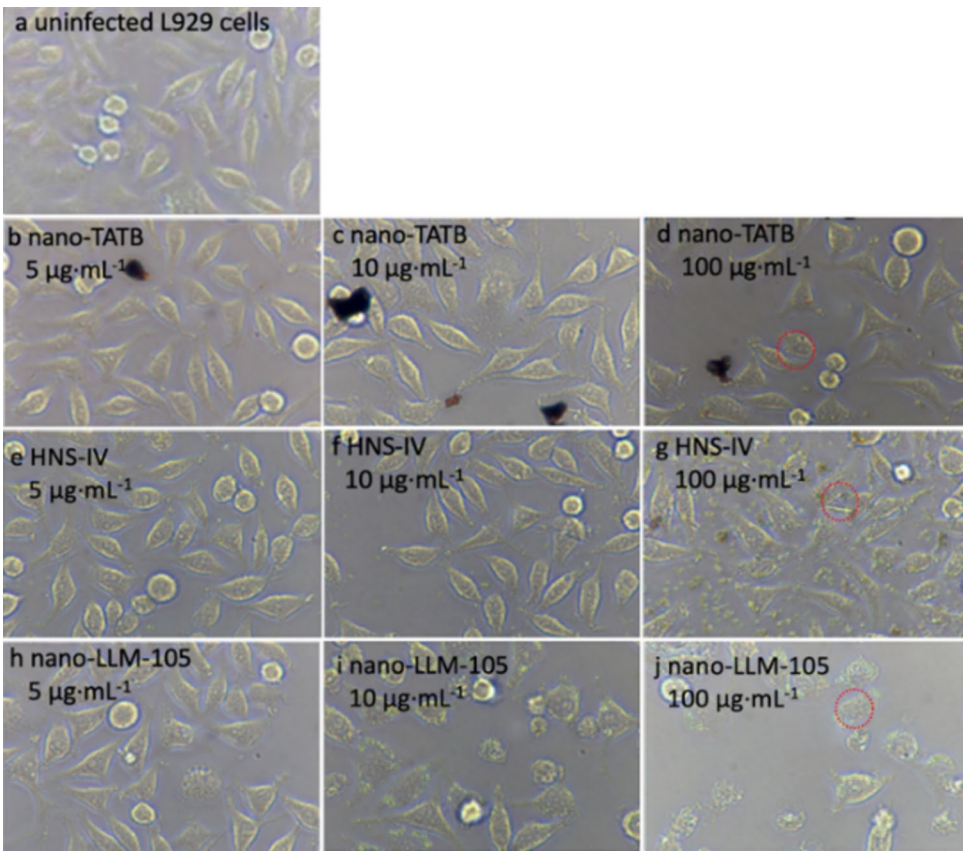

Fig. 1 Morphological of uninfected (**a**), and nanoscale EMs stained (**b**–**j**) L929 cells (×400). The red circles in the figure indicate the cell morphology that changed significantly. Note that the cell morphology all changed to different degrees with the increase of EM concentration

morphology of some cells in the nano-LLM-105 contaminated group also changed from a strip with clear shape borders to a round shape with blurred borders (Fig. 1i).

After using a high concentration (100 μg mL^{-1}), the density of L929 cells in the nano-TATB (Fig. 1d) and nano-LLM-105 (Fig. 1j) contaminated groups decreased significantly, and the cell morphology became round with larger cell gaps as shown by the red circles in the figure. The cell density in the HNS-IV (Fig. 1g) contaminated group decreased the most, and almost all cell morphologies showed irregular shapes. Changes in cell morphology were evident, with more spillage and an increased percentage of necrotic cells, indicating significant toxicity of the material at high concentrations.

Effect on cell activity

In vitro cytotoxicity assays are often used to predict the toxicity of a chemical material to an organism. Cell viability was determined by the CCK8 method at different concentrations of EMs after 24 h. Figure 2 shows the effect of nano-TATB, HNS-IV, and nano-LLM-105 on the activity of L929 fibroblasts, which showed a significant dose–effect relationship with the increase in the concentration of different EMs. Still, there were substantial differences in the magnitude of the toxic effects of the three explosives. As the concentration of nano-LLM-105 increased from 5 to 250 μg mL^{-1}, the activity of L929 cells decreased by nearly half, indicating that nano-LLM-105 is highly cytotoxic. It is clear from the graph that nano-LLM-105 has the greatest degree of toxic effect on cells, followed by HNS-IV, and nano-TATB has the weakest toxic effect.

Specifically, around 10 μg mL^{-1}, the cell viability was still high, about 70%, and decreased abruptly to less than 30% around 25 μg mL^{-1}, indicating that nano-LLM-105 staining significantly reduced cell activity and inhibited cell growth in a dose-dependent manner. HNS-IV was less toxic to L929 cells at a concentration of 25 μg mL^{-1}, with cell activity above 80%, and the cell survival rate was (59.34 ± 4.48)% at 250 μg mL^{-1}. At the maximum concentration of 250 μg-mL^{-1} of nano-TATB, the cell survival rate was still (74.38 ± 2.77) %, and the inhibition of cell activity was not obvious at such a high concentration, indicating that the toxicity of nano-TATB and HNS-IV to L929 cells was very low. According to the dose relationship in Fig. 2c, the half maximal inhibitory concentration (IC_{50}) value of nano-LLM-105 own L929 cells at 24 h was calculated to be 15.74 μg mL^{-1}. However, for nano-TATB and HNS-IV, the inhibition was not less than 50% even at a high concentration of 250 μg-mL^{-1}, so it was impossible to obtain, and it was not necessary to require their $IC_{50.}$

Effect on cell membrane permeability

Lactate dehydrogenase activity is elevated in many pathological states, as shown in Fig. 3. When L929 cells were incubated with the three groups of EMs, the LDH activity in the cell supernatant was found to increase with increasing concentrations of nano-TATB, HNS-IV, and nano-LLM-105 compared to the blank control in each group, indicating an increase in cell membrane permeability, but the degree of change was different for the three materials. Among them, HNS-IV (Fig. 3b) triggered the release of large amounts of LDH from the cells, indicating that the integrity of the L929 cells membrane was lost, which increased its permeability. Cell death caused by the disruption of cell membranes is one of the standard mechanisms for the cytotoxicity of NMs. It has been shown that elevated serum LDH is an independent risk factor for the severity of COVID-19 pathogenesis and mortality (Li et al. 2020). High LDH activity in sickle cell disease (SCD) arises from multiple mechanisms, particularly intravascular hemolysis, ischemia–reperfusion injury, and

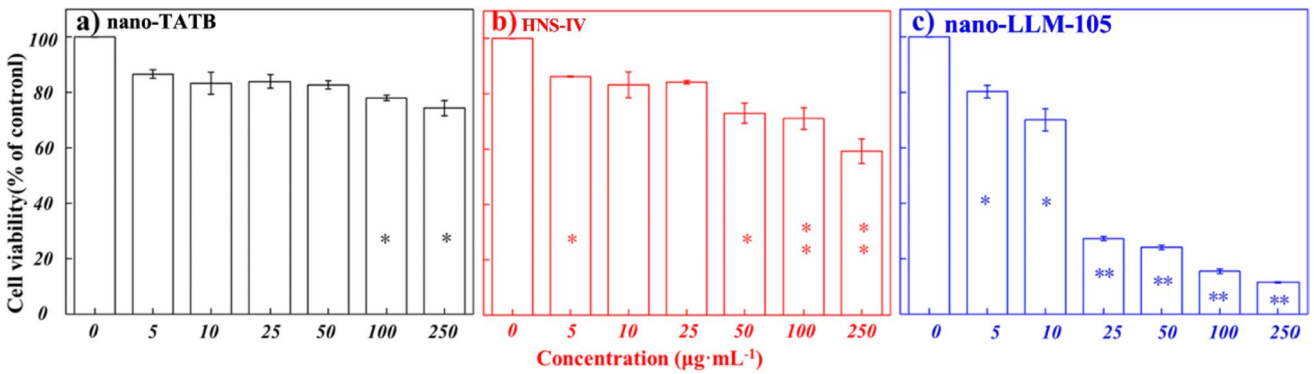

Fig. 2 Effect of three nanoscale EMs on the viability of L929 cells at different dyeing doses. Note that the cellular activity all showed different degrees of diminution with increasing concentration of EMs. And according to the trend nano-LLM-105 has the strongest cytotoxic effect, followed by HNS-IV, and nano-TATB has the weakest effect

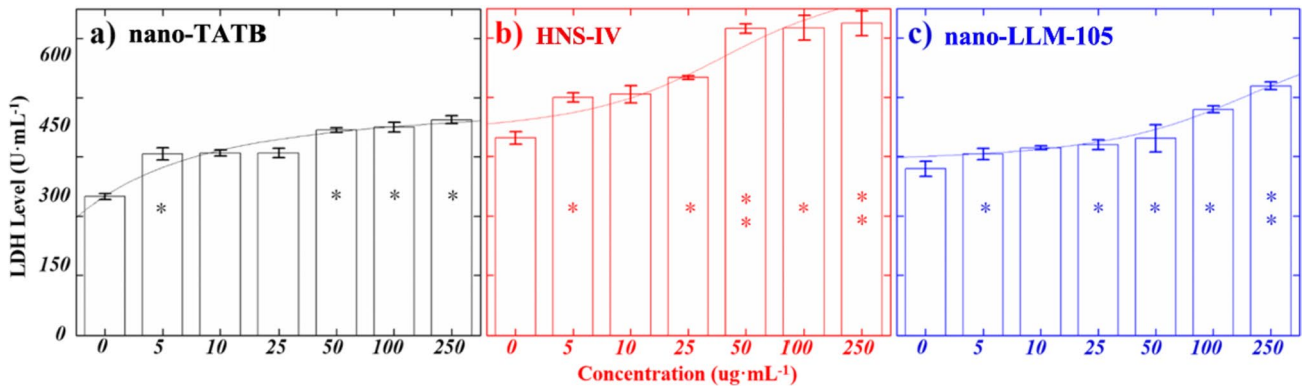

Fig. 3 Effect of three nano energetic materials on the integrity of L929 cells membrane at different doses (*P < 0.05, **P < 0.01). Elevated LDH levels indicated that the L929 cell membrane was fragmented, with HNS-IV having the strongest membrane-disrupting effect

tissue necrosis (Stankovic Stojanovic and Lionnet 2016). Ahamed et al. exposed lung A549 cells to 50 µg/mL CeO_2 NPs, reduced graphene oxide (RGO), and CeO_2-RGO nanocomposites for 24 h and found that RGO significantly induced LDH leakage and that cytosolic LDH leakage into the medium was an indicator of cell membrane damage (Ahamed et al. 2019).

Cellular oxidative stress levels

Reactive oxygen species (ROS) are notable species of free radicals in living organisms. When organisms are exposed to external environmental stresses, such as pollutant exposure, this can lead to the production of large amounts of exogenous ROS, such as superoxide anion ($O_2\bullet^-$), hydroxyl radical ($HO\bullet^-$) that can act as signaling molecules during apoptosis (Nel et al. 2006). In contrast, biological organisms have a set of antioxidant defense systems that eliminate free radicals, such as superoxide dismutase (SOD), whose activity changes in response to the level of ROS in the body.

Oxidative stress is a possible mechanism for the potential toxicity of NMs, causing cellular necrosis (Dusinska et al. 2017). Nanoscale materials may induce oxidative stress through the production of pro-oxidants or the reduction of antioxidants. Specifically, the generation of intracellular ROS or the depletion of antioxidants may lead to oxidative damage to cellular biomolecules. Moreover, ROS can initiate a chain reaction that readily reacts with various unsaturated fatty acids and cholesterol on the cell membrane, and this direct oxidative damage to the cell can lead to apoptosis. It has been reported that curcumin regulation of nuclear transcription factor κB (NF-κB) activity is affected by ROS in transformed cells, and abnormal κB activity induces apoptosis (Chi et al. 2018; Deragon et al. 2020). Paclitaxel diketone induces apoptosis in BCR-ABL-positive cells through the generation of ROS by the mechanism of mitochondria-mediated apoptosis (Uchihara et al. 2018).

As shown in Fig. 4, the HNS-IV and nano-TATB-dyed groups caused almost no significant changes in intracellular SOD activity, which was not statistically significant. In contrast, the SOD activity of the nano-LLM-105-tainted group decreased with the increase of the dose; the intracellular SOD activity significantly reduced at the concentration of nano-LLM-105 above 25 µg mL^{-1}. The decrease in SOD activity indicates that its ability to scavenge ROS is diminished, and the excess of free radicals will oxidize unsaturated fatty acids in the biofilm to damage the cell membrane structure, resulting in a decrease in cell activity.

Several studies have also demonstrated this mechanism. Ahamed et al. found that reduced RGO NMs significantly induced reactive oxygen species (ROS) production and

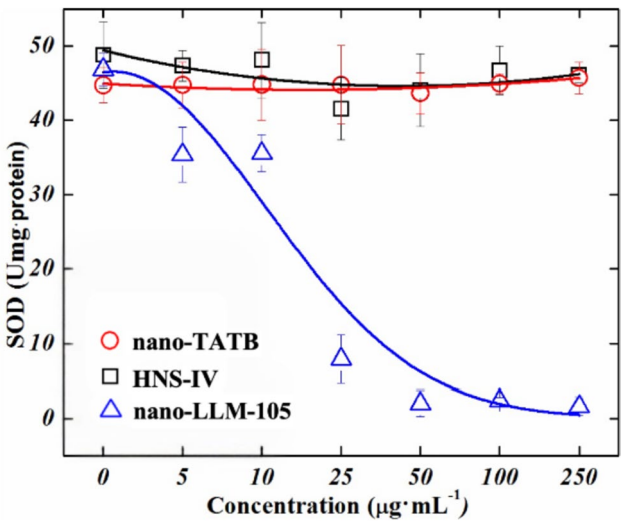

Fig. 4 Effect of three nanoscale energetic material on the intracellular SOD activity of L929 cells at different dyeing doses. The decline in SOD activity indicates a reduced ability to scavenge ROS. The toxicity mechanism of nano-LLM-105 is mainly manifested by oxidative stress

reduced glutathione levels in human lung epithelial A549 cells (Ahamed et al. 2019). Shaheen et al. investigated the induction of oxidative stress-mediated toxicity in graphene oxide (GO) ZnO nanocomposites in MCF-7 cells (Shaheen et al. 2018). CuO NPs in A549 cells induced cytotoxicity, oxidative stress, and severe ultrastructural damage (Moschini et al. 2013). Rao et al. found that the toxic effects of nano-hydroxyapatite HAP on renal epithelial cells were mainly attributed to its entry into the cells through endocytosis and accumulation in the lysosomes, leading to increased intracellular reactive oxygen species (ROS) levels and disruption of lysosomal integrity (Rao et al. 2019).

Apoptosis

Apoptosis is a self-protection mechanism for organisms to clear potential hazards, and oxidative protein damage leading to protein carbonylation is also associated with the generation of apoptosis. Apoptosis, which is closely related to cell proliferation and differentiation, is the main pathological basis of many diseases and one of the most important indicators for drug development and toxicity testing, for example, apoptosis as a parameter was used in the study of the toxicity of secondary effluents disinfected with performic acid (PFA) (Ragazzo et al. 2017). It has been reported that furan can produce cytotoxic effects on Leydig cells through DNA damage and apoptosis (Yilmaz et al. 2023). The study of the mechanism of toxicant-induced apoptosis is essential for comparing the toxicity of different toxicants and understanding their toxicological characteristics. In this paper, we carry out a simple verification that the toxicity of nanomaterials induces apoptosis, and its specific mechanism still needs to be continued to explore.

As shown in Table 1, the apoptosis percentages of nano-TATB, HNS-IV, and nano-LLM-105 NMs at different concentrations showed a dose-dependent apoptosis level with increasing attention. When the concentration of nano-LLM-105 (Fig. 5) was 10 μg mL^{-1}, the images were significantly dispersed when comparing the responses at low concentrations, indicating that it promoted apoptosis. As the concentration was increased to 100 μg mL^{-1}, the level of apoptosis was nearly half. This suggests that nano-LLM-105

Table 1 Effects of nano-TATB, HNS-IV, and nano-LLM-105 on the apoptosis level of L929 cells

Group	Apoptosis %		
	Nano-TATB	HNS-IV	Nano-LLM-105
Blank	1.88	1.88	1.88
5 μg·mL^{-1}	8.46 ± 0.79	4.52 ± 0.4 7	6. 26 ± 0.33
10 μg·mL^{-1}	8.53 ± 0.35	5.54 ± 0.43	22.69 ± 0.26
100 μg·mL^{-1}	16.46 ± 0.34	8.26 ± 0.27	42.35 ± 1.26

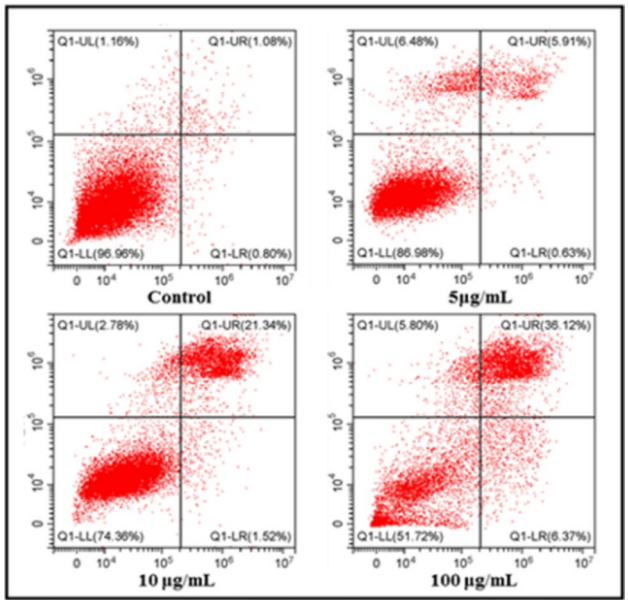

Fig. 5 Effects of nano-LLM-105 at different exposure doses on apoptosis of L929 cells

significantly promoted apoptosis, while HNS-IV and nano-TATB showed apoptosis-inducing effects only at high concentrations; HNS-IV and nano-TATB images are shown in the Supplementary Materials of Fig. S2. This is consistent with the results of cell viability studies, which showed that nano-LLM-105 had the most potent toxic effect, and the decrease in cell viability increased with increasing concentrations. It had the most powerful impact on apoptosis levels. Another study showed a correlation between reduced cell viability and cell membrane rupture, which can be caused by cell gangrene or apoptosis, especially in the middle and late stages of apoptosis (Bao et al. 2015). This suggests that nano-LLM-105 exerts its toxic effects by inducing apoptosis, and thus reduces the viability of the cells.

Conclusion

Energetic materials (EMs) have the potential to cause toxic effects in various tissues and organs, including the liver and kidneys, and may even be teratogenic and mutagenic. The three materials evaluated in this study are among the most promising explosives for industrial applications in the field of EMs, and their cytotoxicity was investigated to assess their potential health risks.

In this experiment, mouse fibroblasts L929 were used as the test cells, and the toxic effects of the nano-sized energetic materials nano-TATB, HNS-IV, and nano-LLM-105 were investigated. The results showed that all three EMs had cytotoxic effects on L929 cells, with nano-LLM-105 being the

most toxic. The toxicity of the nano-LLM-105-treated cells increased with increasing particle concentration, indicating a dose-dependent effect. The half-maximum inhibitory concentration (IC_{50}) of nano-LLM-105 on L929 cells was 15.47 μg mL^{-1}, which was significantly lower than the IC_{50}s of HNS-IV and nano-TATB on L929 cells (> 250 μg mL^{-1}).

The mechanism of cytotoxicity was investigated by measuring cell morphology changes, cell membrane damage, and oxidative stress. The results showed that all three EMs induced cell morphology changes, increased lactate dehydrogenase (LDH) activity, and decreased superoxide dismutase (SOD) activity. These findings suggest that the cytotoxic effects of EMs are mediated by cell membrane damage and oxidative stress.

In conclusion, this study provides valuable insights into the cytotoxic effects of nano-sized energetic materials. The findings suggest that nano-LLM-105 is the most toxic of the three materials evaluated, and that oxidative stress may be a major mechanism of nano-LLM-105 toxicity. These results highlight the need for further research on the toxicological effects of EMs and the development of safer alternative materials.

Supplementary Information The online version contains supplementary material available at https://doi.org/10.1007/s11696-024-03324-6.

Declarations

Conflict of interest The authors declare no conflict of interest.

References

Ahamed M, Akhtar MJ, Khan MAM, Alaizeri ZM, Alhadlaq HA (2019) Evaluation of the cytotoxicity and oxidative stress response of CeO_2-RGO nanocomposites in human lung epithelial A549 cells. Nanomaterials (basel) 9(12):1709. https://doi.org/10.3390/nano9121709

Atalay H, Celi KA, Ayaz F (2018) Investigation of genotoxic and apoptotic effects of zirconium oxide nanoparticles (20nm) on L929 Mouse fibroblast cell line. Chem Biol Interact 296:98–104. https://doi.org/10.1016/j.cbi.2018.09.017

Badgujar DM, Talawar MB, Asthana SN, Mahulikar PP (2008) Advances in science and technology of modern energetic materials: an overview. J Hazard Mater 151(2–3):289–305. https://doi.org/10.1016/j.jhazmat.2007.10.039

Banerjee H, Hawkins Z, Dutta S, Smoot D (2003) Effects of 2-amino-4,6-dinitrotoluene on P53 tumor suppressor gene expression. Mol Cell Biochem 252:387–389. https://doi.org/10.1023/A:1025542429071

Bao H, Yu X, Xu C, Li X, Li Z, Wei D, Liu Y (2015) New toxicity mechanism of silver nanoparticles: promoting apoptosis and inhibiting proliferation. PLoS ONE 10(3):e0122535. https://doi.org/10.1371/journal.pone.0122535

Berthelot Y, Valton E, Auroy A, Trottier B, Robidoux PY (2008) Integration of toxicological and chemical tools to assess the bioavailability of metals and energetic compounds in contaminated soils. Chemosphere 74(1):166–177. https://doi.org/10.1016/j.chemosphere.2008.07.056

Can T, Bing H, Liu L (2020) Cytotoxicity and mechanisms of nanoscale HNS, TATB and LLM-105 to RAW264.7. Chin J of Energ Mater 28:792–797. https://doi.org/10.11943/CJEM2020018

Chatterjee A, Thanneeru R, Saha A, Guthikonda KK (2024) Photodegradation of toxic malachite green dye by ZnO and ZnO/SiO_2 nanocomposites under solar radiation: a green practice. Chem Pap. https://doi.org/10.1007/s11696-023-03238-9

Chi J, Yu S, Liu C, Zhao X, Zhong J, Liang Y, Ta N, Yin X, Zhao D (2018) Nox4-dependent ROS production is involved in CVB(3)-induced myocardial apoptosis. Biochem Biophys Res Commun 503(3):1641–1644. https://doi.org/10.1016/j.bbrc.2018.07.093

De Matteis V, Cascione M, De Luca A, Manno DE, Rinaldi R (2022) High doses of silica nanoparticles obtained by microemulsion and green routes compromise human alveolar cells morphology and stiffness differently. Bioinorg Chem Appl 2022:2343167. https://doi.org/10.1155/2022/2343167

Deragon MA, McCaig WD, Patel PS, Haluska RJ, Hodges AL, Sosunov SA, Murphy MP, Ten VS, LaRocca TJ (2020) Mitochondrial ROS prime the hyperglycemic shift from apoptosis to necroptosis. Cell Death Discov 6(1):132. https://doi.org/10.1038/s41420-020-00370-3

Dev A, Srivastava AK, Karmakar S (2017) Nanomaterial toxicity for plants. Environ Chem Lett 16(1):85–100. https://doi.org/10.1007/s10311-017-0667-6

Du Y, Qu Z, Wang H, Cui H, Wang X (2021) Review on the synthesis and performance for 1,3,4-oxadiazole-based energetic materials. Propellants Explos Pyrotech 46(6):860–874. https://doi.org/10.1002/prep.202000318

Dusinska M, Tulinska J, El Yamani N, Kuricova M, Liskova A, Rollerova E, Runden-Pran E, Smolkova B (2017) Immunotoxicity, genotoxicity and epigenetic toxicity of nanomaterials: new strategies for toxicity testing? Food Chem Toxicol 109:797–811. https://doi.org/10.1016/j.fct.2017.08.030

Finkel T, Holbrook NJ (2000) Oxidants, oxidative stress and the biology of ageing. Nature 408(6809):239–247. https://doi.org/10.1038/35041687

Franklin RA (2021) Fibroblasts and macrophages: collaborators in tissue homeostasis. Immunol Rev 302(1):86–103. https://doi.org/10.1111/imr.12989

Gao H, Zhang Q, Shreeve JM (2020) Fused heterocycle-based energetic materials (2012–2019). J of Mater Chem A 8(8):4193–4216. https://doi.org/10.1039/c9ta12704f

Hartwig A, van Thriel C (2023) Risk assessment of nanomaterials toxicity. Nanomaterials (basel) 13(9):1512. https://doi.org/10.3390/nano13091512

He F, Zhu X, Huang Y (1999) Construction and application of L929 cell model expressing human Bcl-2 protein. Chin Sci Bull 44(12):1095–1098. https://doi.org/10.1007/BF02886133

Honeycutt ME, Jarvis AS, McFarland VA (1996) Cytotoxicity and Mutagenicity of 2,4,6-trinitrotoluene and Its Metabolites. Ecotox Environ Safe 35(3):282–287. https://doi.org/10.1006/eesa.1996.0112

Johnson MS, Eck WS, Lent EM (2017) Toxicity of insensitive munition (IMX) formulations and components. Propellants Explos Pyrotech 42(1):9–16. https://doi.org/10.1002/prep.201600147

Kim TH, Kim M, Park HS, Shin US, Gong MS, Kim HW (2012) Size-dependent cellular toxicity of silver nanoparticles. J Biomed Mater Res A 100(4):1033–1043. https://doi.org/10.1002/jbm.a.34053

Klapötke TM, Scharf R, Stierstorfer J, Unger CC (2020) Toxicity assessment of energetic materials by using the luminescent bacteria inhibition test. Propellants Explos Pyrotech 46(1):114–123. https://doi.org/10.1002/prep.202000044

Lachance B, Robidoux PY, Hawari J, Ampleman G, Thiboutot S, Sunahara GI (1999) Cytotoxic and genotoxic effects of energetic compounds on bacterial and mammalian cells in vitro. Mutat

Res-Genet Toxicol Environ Mutagen 444(1):25–39. https://doi.org/10.1016/S1383-5718(99)00073-X

Li C, Ye JF, Chen QJ, Hu WH, Wang LL, Fan YM, Lu ZJ, Chen J, Chen ZS, Chen SY, Tong JL, Xiaol W, Mei J, Lu HY (2020) Elevated lactate dehydrogenase (LDH) level as an independent risk factor for the severity and mortality of COVID-19. Aging-Us 12(15):15670–15681. https://doi.org/10.18632/aging.103770

Liu Y, Nie YG, Wang JJ, Wang J, Wang X, Chen SP, Zhao GP, Wu LJ, Xu A (2018) Mechanisms involved in the impact of engineered nanomaterials on the joint toxicity with environmental pollutants. Ecotoxicol Environ Saf 162:92–102. https://doi.org/10.1016/j.ecoenv.2018.06.079

Mohanty S, Patel P, Jha E, Panda PK, Kumari P, Singh S, Sinha A, Saha AK, Kaushik NK, Raina V, Verma SK, Suar M (2022) In vivo intrinsic atomic interaction infer molecular ecotoxicity of industrial TiO_2 nanoparticles via oxidative stress channelized seatosis and apoptosis in paramecium caudatum. Ecotoxicol Environ Saf 241:113708. https://doi.org/10.1016/j.ecoenv.2022.113708

Moschini E, Gualtieri M, Colombo M, Fascio U, Camatini M, Mantecca P (2013) The modality of cell-particle interactions drives the toxicity of nanosized CuO and $TiO_{(2)}$ in human alveolar epithelial cells. Toxicol Lett 222(2):102–116. https://doi.org/10.1016/j.toxlet.2013.07.019

Mu RH, Ye SP, Lin R, Li YP, Guo X, An LP (2022) Effects of peroxiredoxin 6 and its mutants on the isoproterenol induced myocardial injury in H9C2 cells and rats. Oxidative Med Cell Longevity 2022:2576310. https://doi.org/10.1155/2022/2576310

Nel A, Xia T, Madler L, Li N (2006) Toxic Potential of Materials at the Nanolevel. Science 311(5761):622–627. https://doi.org/10.1126/science.1114397

Prasad R (2019a) Approaches in nanoparticles biosynthesis and toxicity. Plant nanobionics, vol 2. Springer, Cham

Prasad R (2019b) Nanotechnology in the life sciences. Microbial nanobionics, vol 1. Springer, Cham

Qu C, Qian S, Chen L, Guan Y, Zheng L, Liu S, Chen W, Cai P, Huang Q (2019) Size-dependent bacterial toxicity of hematite particles. Environ Sci Technol 53(14):8147–8156. https://doi.org/10.1021/acs.est.9b00856

Ragazzo P, Feretti D, Monarca S, Dominici L, Ceretti E, Viola G, Piccolo V, Chiucchini N, Villarini M (2017) Evaluation of cytotoxicity, genotoxicity, and apoptosis of wastewater before and after disinfection with performic acid. Water Res 116:44–52. https://doi.org/10.1016/j.watres.2017.03.016

Rao CY, Sun XY, Ouyang JM (2019) Effects of physical properties of nano-sized hydroxyapatite crystals on cellular toxicity in renal epithelial cells. Mater Sci Eng C Mater Biol Appl 103:109807. https://doi.org/10.1016/j.msec.2019.109807

Shaheen F, Aziz MH, Fatima M, Khan MA, Ahmed F, Ahmad R, Ahmad MA, Alkhuraiji TS, Akram MW, Raza R, Ali SM (2018) In vitro cytotoxicity and morphological assessments of GO-ZnO against the MCF-7 cells: determination of singlet oxygen by chemical trapping. Nanomaterials 8(7):539. https://doi.org/10.3390/nano8070539

Skalska J, Struzynska L (2015) Toxic effects of silver nanoparticles in mammals—does a risk of neurotoxicity exist? Folia Neuropathol 53(4):281–300. https://doi.org/10.5114/fn.2015.56543

Stankovic Stojanovic K, Lionnet F (2016) Lactate dehydrogenase in sickle cell disease. Clin Chim Acta 458:99–102. https://doi.org/10.1016/j.cca.2016.04.035

Uchihara Y, Tago K, Taguchi H, Narukawa Y, Kiuchi F, Tamura H, Funakoshi-Tago M (2018) Taxodione induces apoptosis in BCR-ABL-positive cells through ROS generation. Biochem Pharmacol 154:357–372. https://doi.org/10.1016/j.bcp.2018.05.018

Vimbela GV, Ngo SM, Fraze C, Yang L, Stout DA (2017) Antibacterial properties and toxicity from metallic nanomaterials. Int J Nanomed 12:3941–3965. https://doi.org/10.2147/IJN.S134526

Wang P, Qin D, Chen Y, Xin F, Liang Y, Liu C (2001) Stuy on the Preparation Technology of Ultrafine HNS. Energetic Materials 9:153–155

Wang L, Murphy-Ullrich JE, Song Y (2019) Multiscale simulation of the interaction of calreticulin-thrombospondin-1 complex with a model membrane microdomain. J Biomol Struct Dyn 37(3):811–822. https://doi.org/10.1080/07391102.2018.1433065

Wang C, Chen L, Xu J, Zhang L, Yang X, Zhang X, Zhang C, Gao P, Zhu L (2023) Environmental behaviors and toxic mechanisms of engineered nanomaterials in soil. Environ Res 242:117820. https://doi.org/10.1016/j.envres.2023.117820

Winkless L (2023) Improved toxicity test reveals risk posed by nanomaterials. Mater Today 71:6–7. https://doi.org/10.1016/j.mattod.2023.11.024

Wu GZ, Huang Y, Li J, Lu YY, Liu L, Du DL, Xue YL (2022) Chronic level of exposures to low-dosed MoS_2 nanomaterials exhibits more toxic effects in HaCaT keratinocytes. Ecotox Environ Safe 242:113848. https://doi.org/10.1016/j.ecoenv.2022.113848

Yang GC, Nie FD, Huang H, Zhao L, Pang WT (2006) Preparation and characterization of Nano-TATB explosive. Propellants, Explos, Pyrotech 31(5):390–394. https://doi.org/10.1002/prep.200600053

Yang X, Lai JL, Zhang Y, Luo XG, Han MW, Zhao SP (2021) Microbial community structure and metabolome profiling characteristics of soil contaminated by TNT, RDX, and HMX. Environ Pollut 285:117478. https://doi.org/10.1016/j.envpol.2021.117478

Yilmaz B, Aydin Y, Orta-Yilmaz B (2023) Furan promotes cytotoxic effects through DNA damage and cell apoptosis in Leydig cells. Toxicol Mech Methods 33:796–805. https://doi.org/10.1080/15376516.2023.2240884

Zhang J, Wu P, Yang Z, Gao B, Zhang J, Wang P, Nie F, Liao L (2014) Preparation and properties of submicrometer-sized LLM-105 via spray-crystallization method. Propellants, Explos Pyrotech 39(5):653–657. https://doi.org/10.1002/prep.201300174